

# Monodisperse Bismuth-Halide Double Perovskite Nanocrystals Confined in Mesoporous Silica Templates

*Yue-Qiao Hu,\* Li-Juan Fan, Hong-Yan Hui, Hong-Qiang Wen, De-Suo Yang,\*  
Guo-Dong Feng\**

Key Laboratory of Advanced Molecular Engineering Materials, College of Chemistry  
and Chemical Engineering, Baoji University of Arts and Sciences, Baoji 721013,  
China. No. 1, Hi-Tech Avenue, Baoji

## Synthesis of mesoporous silica templates

**KIT-6** A mixture of 2 g P123 (Aldrich,  $\text{EO}_{20}\text{PO}_{70}\text{EO}_{20}$ ,  $M_n=5800$ ), 5 ml (12 M) HCl and 108.5 ml water was stirred well in a beaker at room temperature (35 °C). Then, 3.75 ml *N*-butyl alcohol was added and continuous stirred for 1 h before adding 6.9 ml TEOS, and the second mixture was stirred for 24 h at 35 °C before transferring into a Teflon bottle and heating at 100 °C for 24 h in the oven. The final product was got by filtering, washing with water, drying at room temperature and calcining in muffle furnace at 550 °C for 6 h.

**SBA-15** 4.0 g P123 was dissolved by stirring vigorously in a solution of 126 mL deionized water and 24 ml (2 M) HCl, then 9.2 ml TEOS was added into the solution. After stirring for 24 h at 40 °C, the mixture was transferred into a Teflon bottle and heated at 100 °C for 24 h. After the reaction, the product was filtered, washed with water and dried at 60 °C, and then calcined in muffle furnace at 550 °C.

**MCM-41** 2 g CTAB was dissolved in a solution of 100 ml water and 8.8 ml 45%  $\text{NH}_3 \cdot \text{H}_2\text{O}$ , then 8.3 ml TEOS was injected into the mixture with an injection pump for 1 h. The solution was stirred for 24 h at room temperature, the gel solution was transferred into a Teflon bottle and crystallized at 100 °C for 24 h. Finally, the product was obtained through filtering, washing with water, drying at 60 °C and calcining in muffle furnace at 550 °C for 6 h.

The phase and purity of above three templates were proved by SAXS data in Figure S4-6, their BET surface and pore size were carried out by physical adsorption/desorption experiments in Figure S7-12.

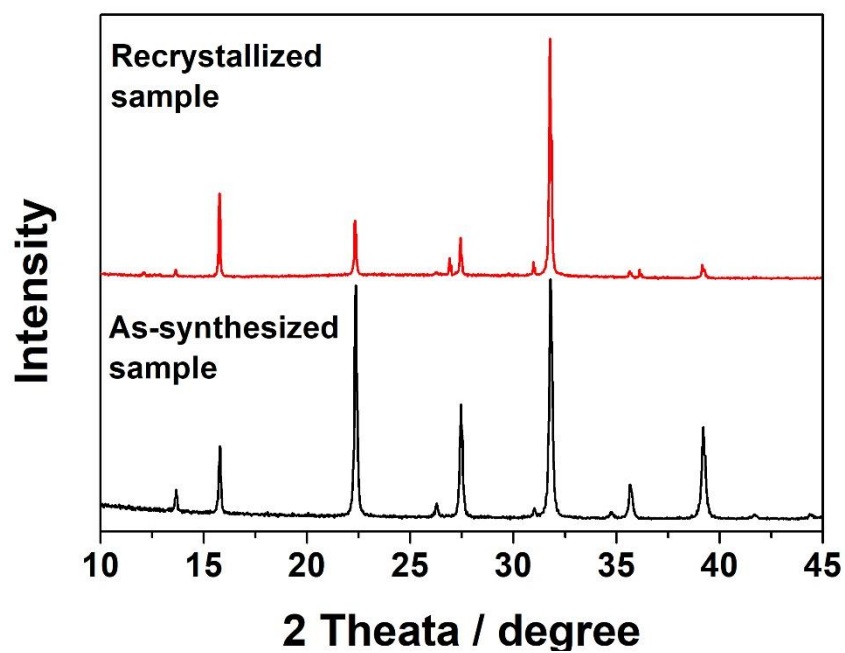


**Figure S1.** PXRD of the as-synthesized and recrystallized samples of **1**.

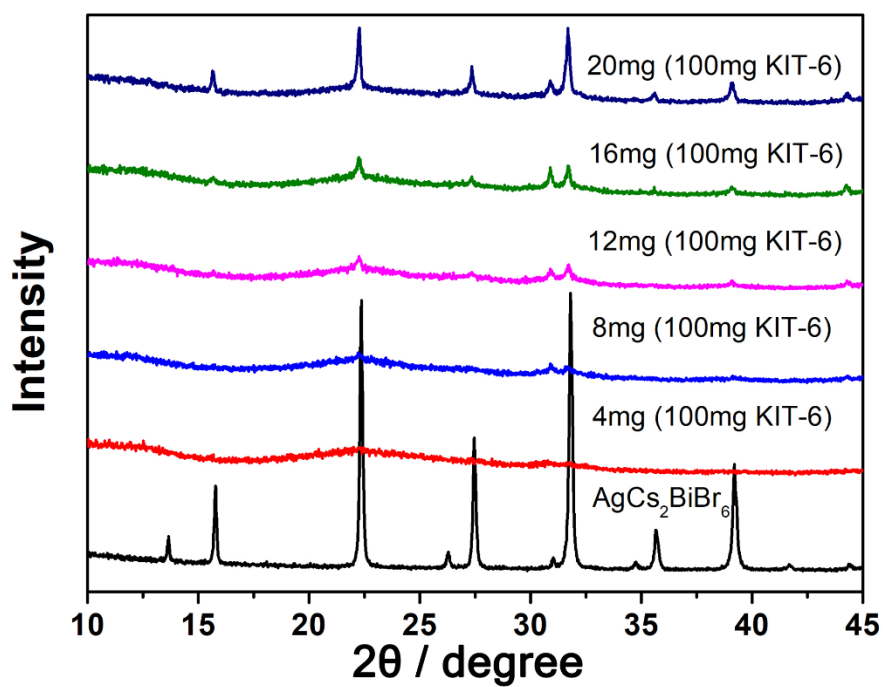


**Figure S2.** PXRD of 1@KIT-6 with different loading amount.

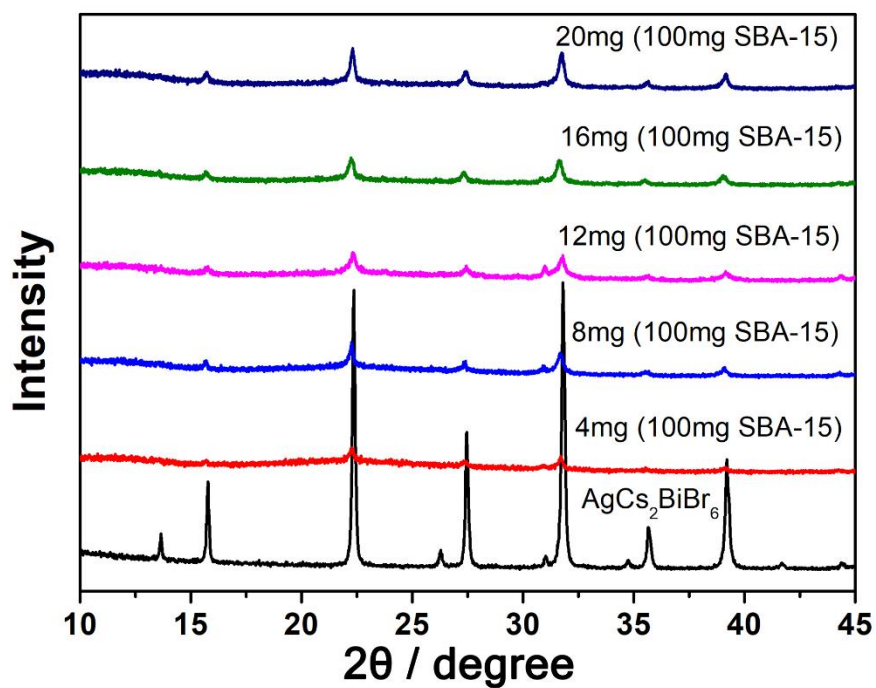


**Figure S3.** PXRD of 1@SBA-15 with different loading amount.

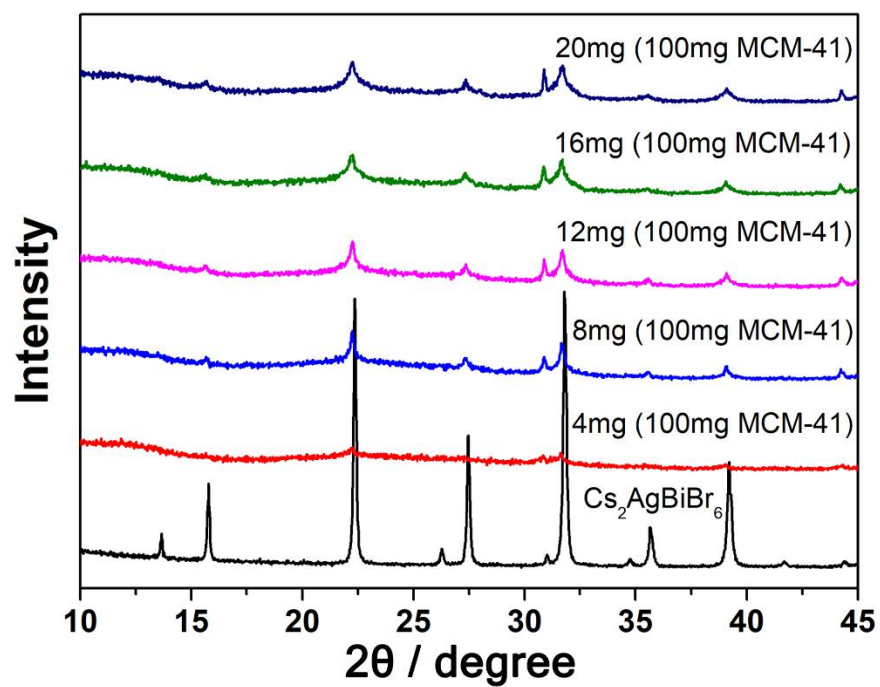


**Figure S4.** PXRD of **1**@MCM-41 with different loading amount.

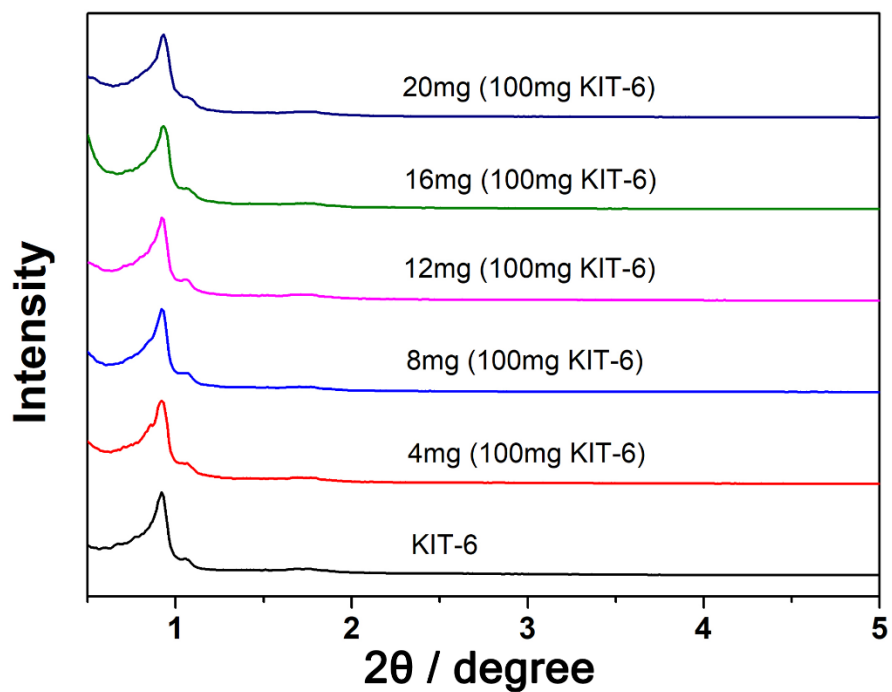


**Figure S5.** SAXS of **1**@KIT-6 with different loading amount.

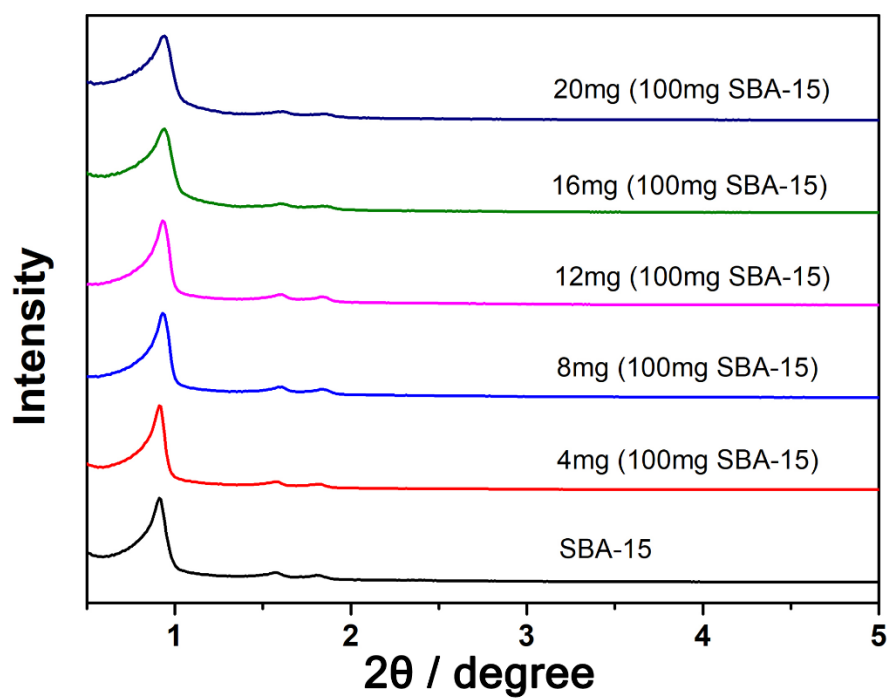


**Figure S6.** SAXS of 1@SBA-15 with different loading amount.

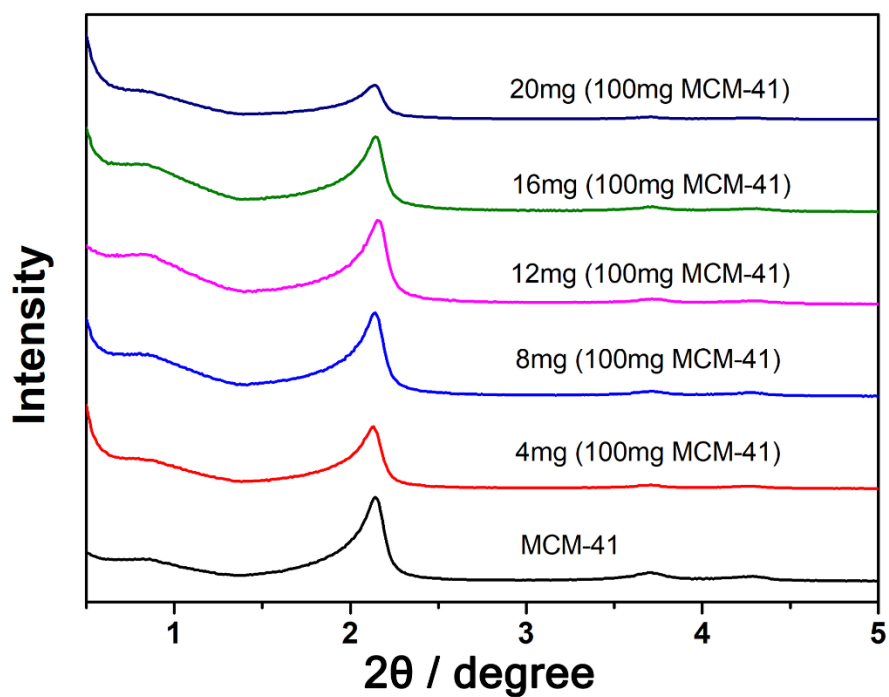


**Figure S7.** SAXS of 1@MCM-41 with different loading amount.

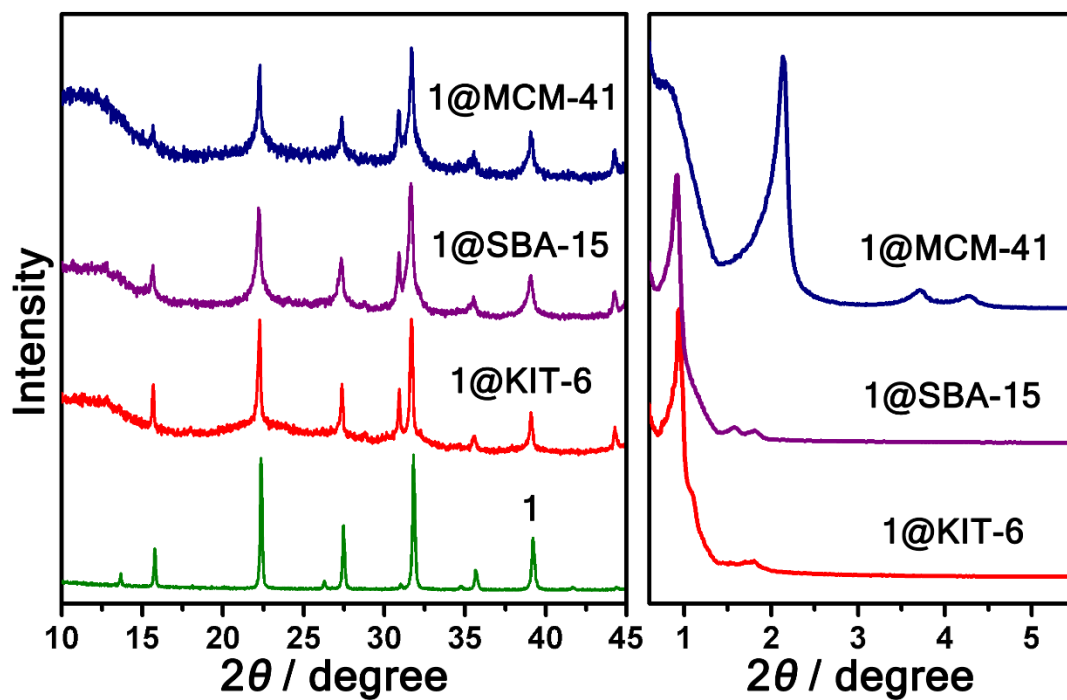


**Figure S8.** Stability of 1@KIT-6, 1@SBA-15, 1@MCM-41. The newly prepared samples were kept in air with relative humidity of 55 % for 180 days, and the PXRD patterns of 1@KIT-6, 1@SBA-15, 1@MCM-41 after moisture showed no evidence of material decomposition, which proves the high stability of the samples.

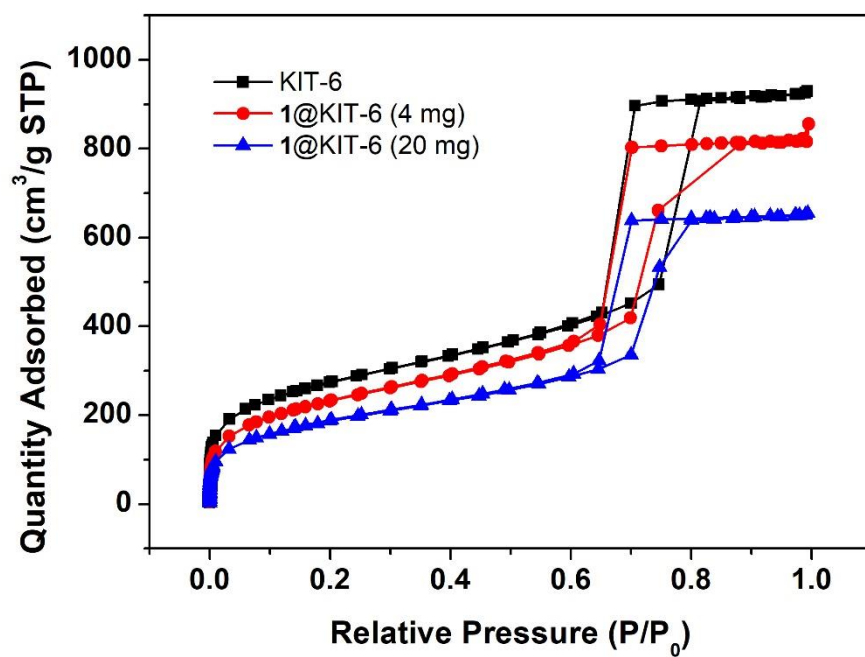


**Figure S9.** N<sub>2</sub> adsorption/desorption data of KIT-6 and **1**@KIT-6 with different loading amount.

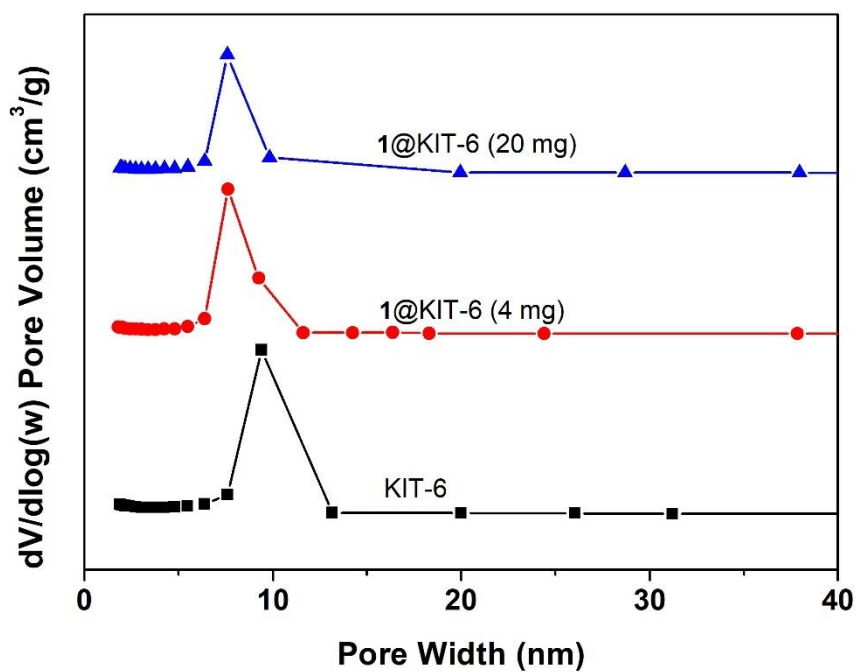


**Figure S10.** Pore size distribution of KIT-6 and **1**@KIT-6 with different loading amount.



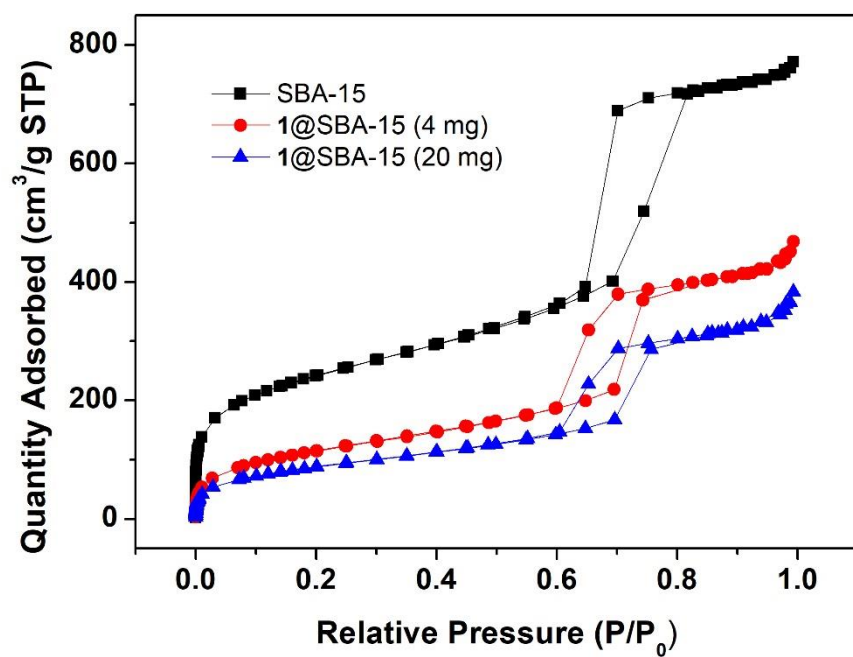


**Figure S11.** N<sub>2</sub> adsorption/desorption data of SBA-15 and **1**@SBA-15 with different loading amount.

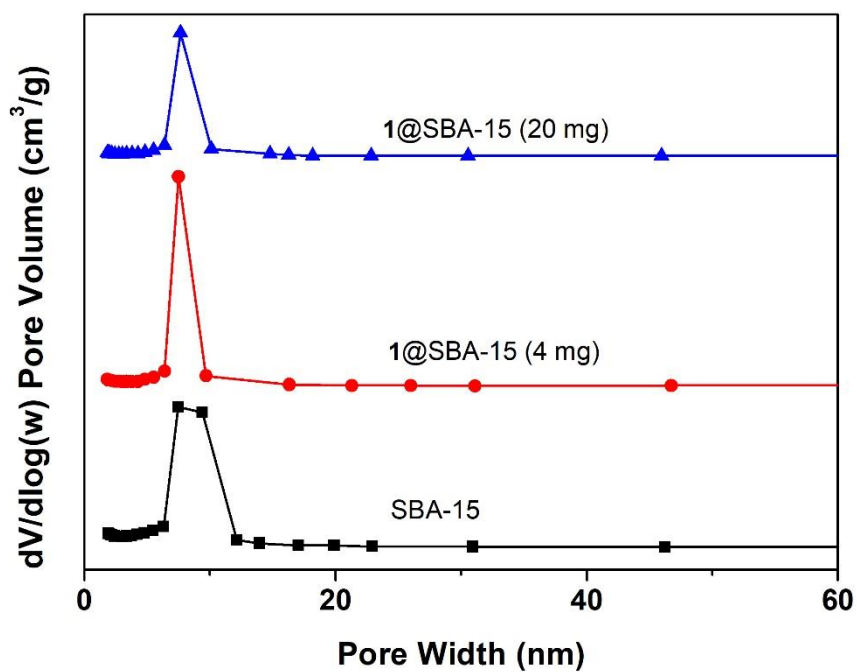


**Figure S12.** Pore size distribution of SBA-15 and **1**@SBA-15 with different loading amount.

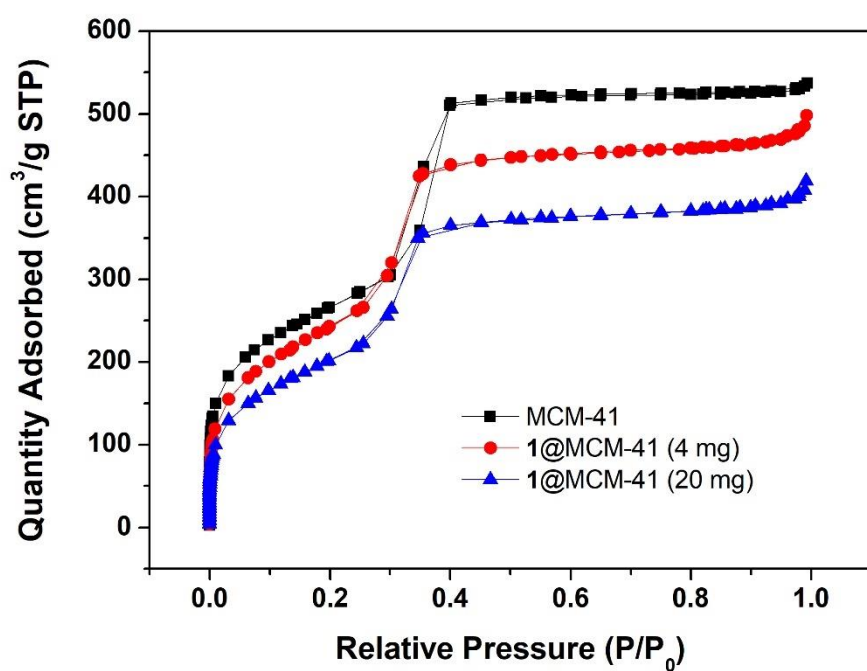


**Figure S13.** N<sub>2</sub> adsorption/desorption data of MCM-41 and **1**@MCM-41 with different loading amount.

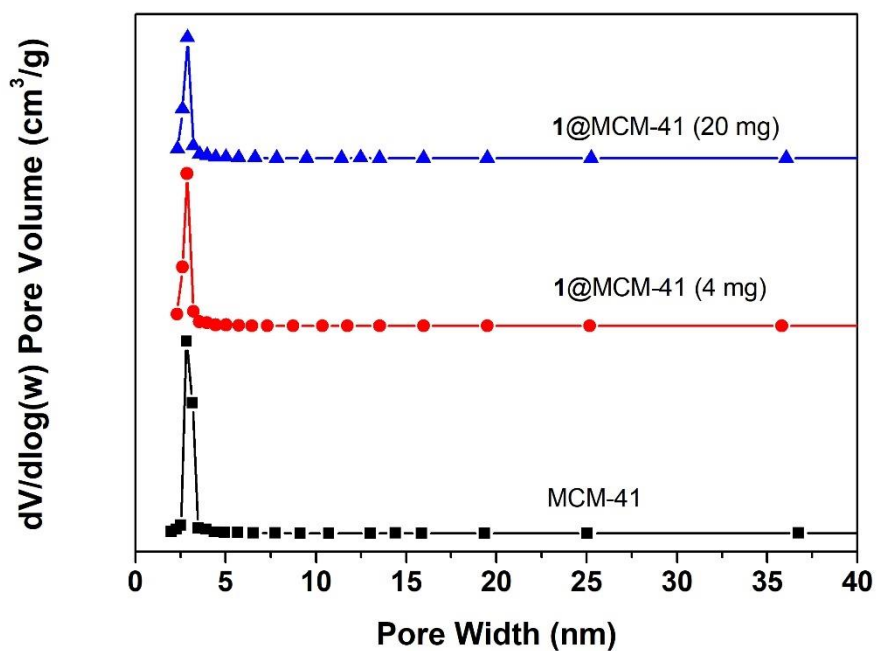


**Figure S14.** Pore size distribution of MCM-41 and **1**@MCM-41 with different loading amount.

**Table S1.** Comparison of specific surface area and pore size of mesoporous silicon before and after loading samples.

| Sample                   | BET surface<br>(m <sup>2</sup> /g) | Pore volume<br>(cm <sup>3</sup> /g) | Pore size<br>(nm) |
|--------------------------|------------------------------------|-------------------------------------|-------------------|
| KIT-6                    | 971                                | 1.44                                | 5.92              |
| <b>1</b> @KIT-6 (4 mg)   | 853                                | 1.33                                | 6.02              |
| <b>1</b> @KIT-6 (20 mg)  | 675                                | 1.01                                | 6.12              |
| SBA-15                   | 857                                | 1.19                                | 5.66              |
| <b>1</b> @SBA-15 (4 mg)  | 530                                | 1.02                                | 5.72              |
| <b>1</b> @SBA-15 (20 mg) | 425                                | 0.81                                | 5.81              |
| MCM-41                   | 954                                | 0.83                                | 2.99              |
| <b>1</b> @MCM-41 (4 mg)  | 852                                | 0.76                                | 3.02              |
| <b>1</b> @MCM-41 (20 mg) | 753                                | 0.72                                | 3.07              |

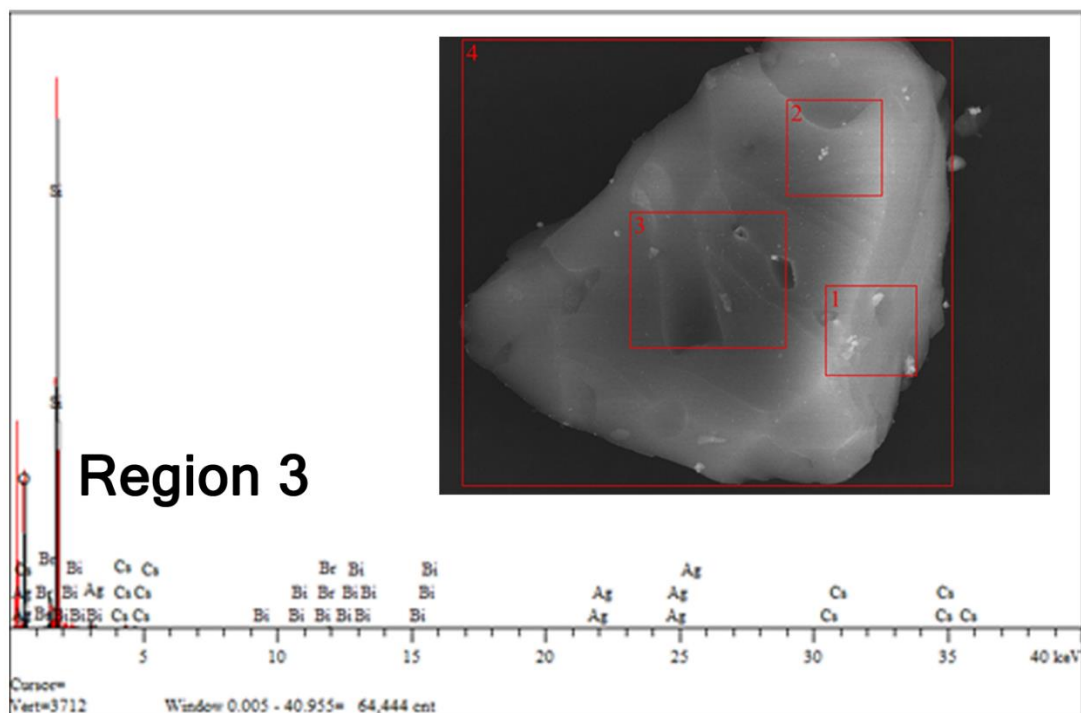


**Figure S15.** EDX image of **1**@KIT-6 (20 mg **1** in 100 mg KIT-6).

**Table S2.** EDX data of **1**@KIT-6 (20 mg **1** in 100 mg KIT-6).

| Element | Region 1<br>Atomic % | Region 2<br>Atomic % | Region 3<br>Atomic % | Region 4<br>Atomic % |
|---------|----------------------|----------------------|----------------------|----------------------|
| Cs      | 0.592                | 0.536                | 0.596                | 0.494                |
| Ag      | 0.255                | 0.252                | 0.304                | 0.249                |
| Bi      | 0.269                | 0.265                | 0.315                | 0.238                |

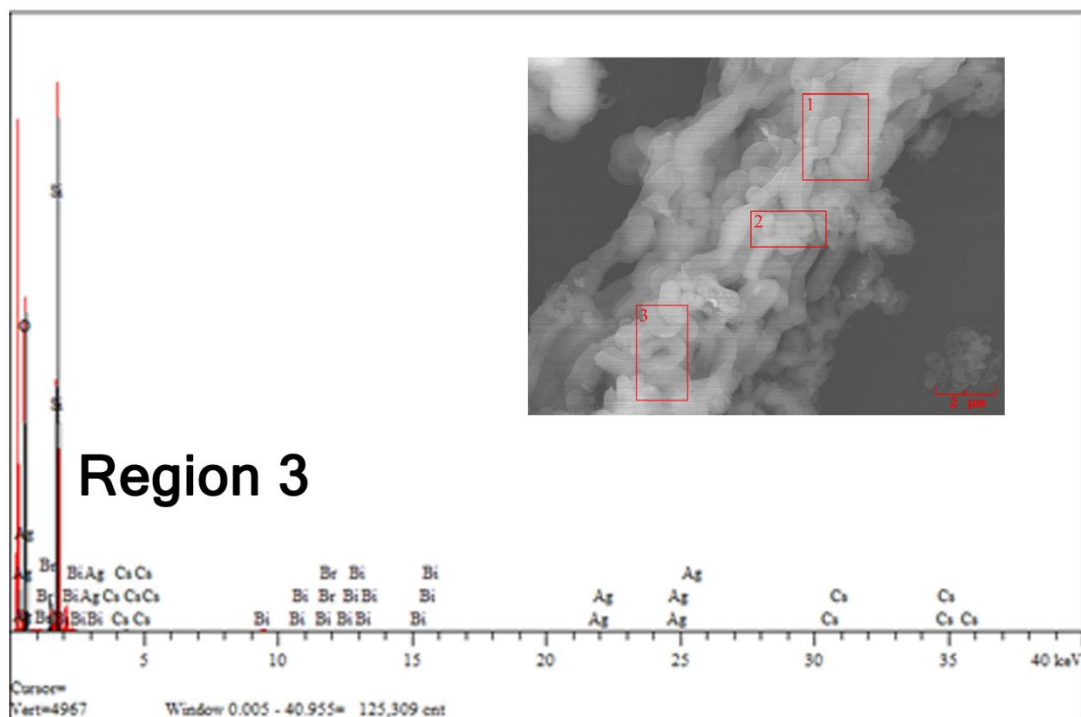


**Figure S16.** EDX image of **1**@SBA-15 (20 mg **1** in 100 mg SBA-15).

**Table S3.** EDX data of **1**@SBA-15 (20 mg **1** in 100 mg SBA-15).

| Element | Region 1<br>Atomic % | Region 2<br>Atomic % | Region 3<br>Atomic % |
|---------|----------------------|----------------------|----------------------|
| Cs      | 0.437                | 0.473                | 0.573                |
| Ag      | 0.211                | 0.244                | 0.273                |
| Bi      | 0.224                | 0.273                | 0.296                |

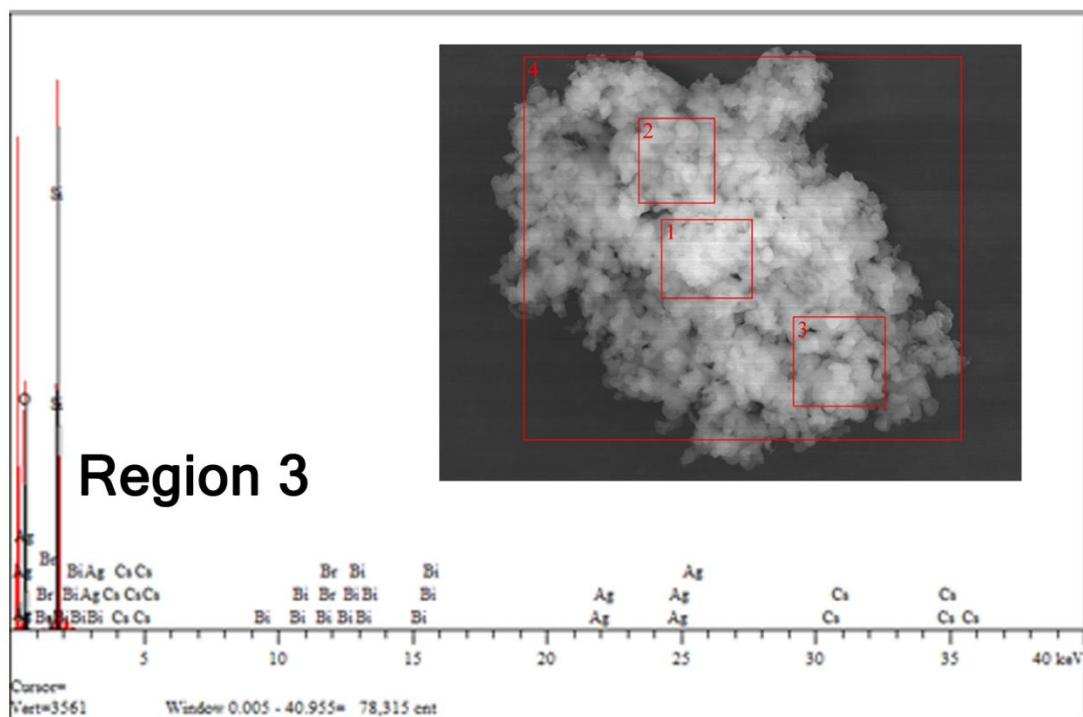


**Figure S17.** EDX image of **1**@MCM-41 (20 mg **1** in 100 mg MCM-41).

**Table S4.** EDX data of **1**@MCM-41 (20 mg **1** in 100 mg MCM-41).

| Element | Region 1<br>Atomic % | Region 2<br>Atomic % | Region 3<br>Atomic % | Region 4<br>Atomic % |
|---------|----------------------|----------------------|----------------------|----------------------|
| Cs      | 0.195                | 0.174                | 0.213                | 0.184                |
| Ag      | 0.111                | 0.089                | 0.104                | 0.106                |
| Bi      | 0.098                | 0.096                | 0.105                | 0.090                |

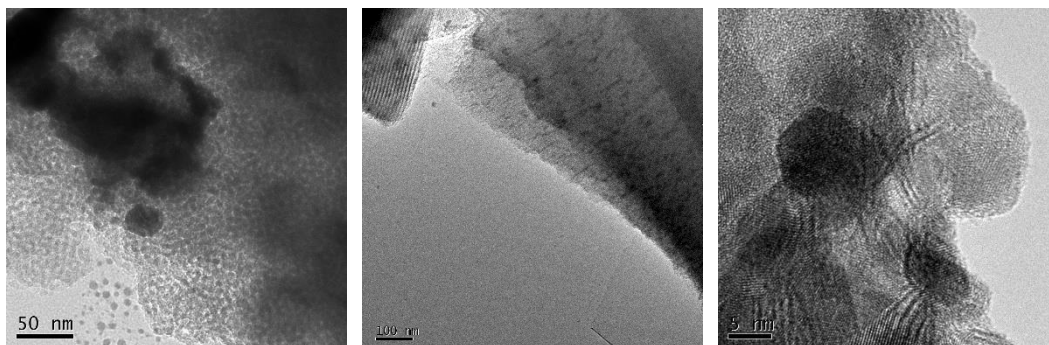


**Figure S18.** TEM images of **1**@KIT-6 (left), **1**@SBA-15 (middle) and **1**@MCM-41 (right). In order to prove the morphology of our samples, we extend the time when the electron beam hit the samples. As shown in Figure S18 left, SiO<sub>2</sub> on KIT-6 will be destroyed or even “dissolved” by long-term electron beam bombardment. However, complex **1**, which is composed of heavy metal ions and halogens, can remain crystalline even after being bombarded by electron beams for a long time. We can see from the figure that there is a clear gap between the nanocrystals of **1**, that is, the destroyed SiO<sub>2</sub>. It can be inferred that the nanocrystals of **1** are monodisperse nanocrystals separated by SiO<sub>2</sub>. At the same time, because SiO<sub>2</sub> is dissolved at the edge of the material, the nanocrystals will detach from the channel, which is just proof of that. For **1**@SBA-15 (Figure S18 middle), we can see in the picture that there are indeed two kinds of nanocrystals: 0D (shorter) and 1D (longer) in the channel of SBA-15. These nanocrystals are separated by SiO<sub>2</sub> and are also monodisperse nanocrystals. For **1**@MCM-41 (Figure S18 right), we can also see that one-dimensional nanocrystals are separated by SiO<sub>2</sub> to form monodisperse 1D nanowires.

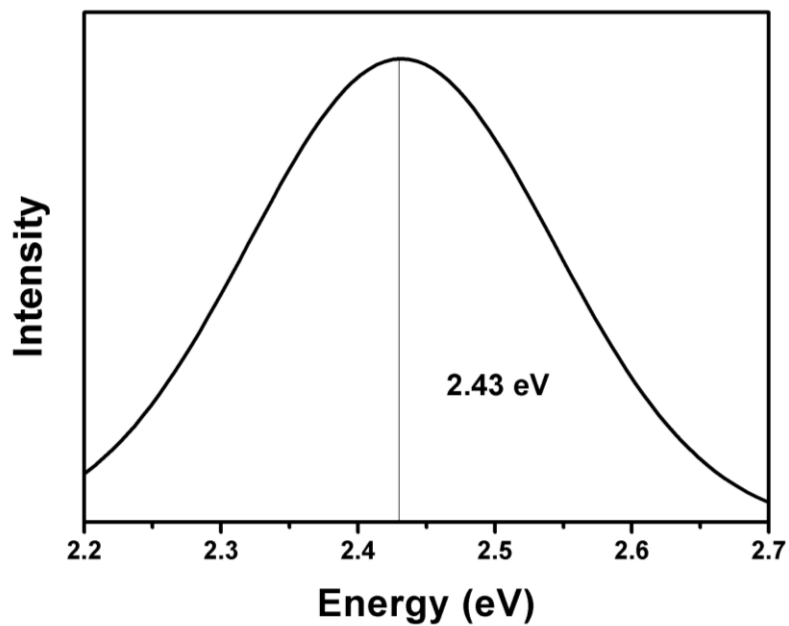


**Figure S19.** PL data of **1**@SBA-15 at 77 K.

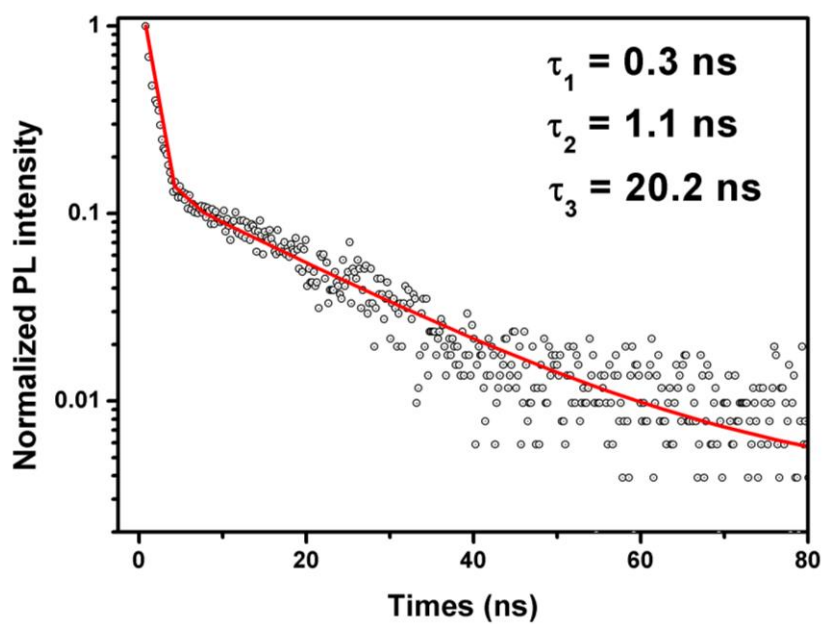


**Figure S20.** Fluorescence lifetime of **1**@SBA-15. This sample have three processes: a short-lifetime process ( $\tau_1 = 0.3$  ns), an intermediate-lifetime process ( $\tau_2 = 1.1$  ns) and a long-lived component ( $\tau_3 = 20.2$  ns).



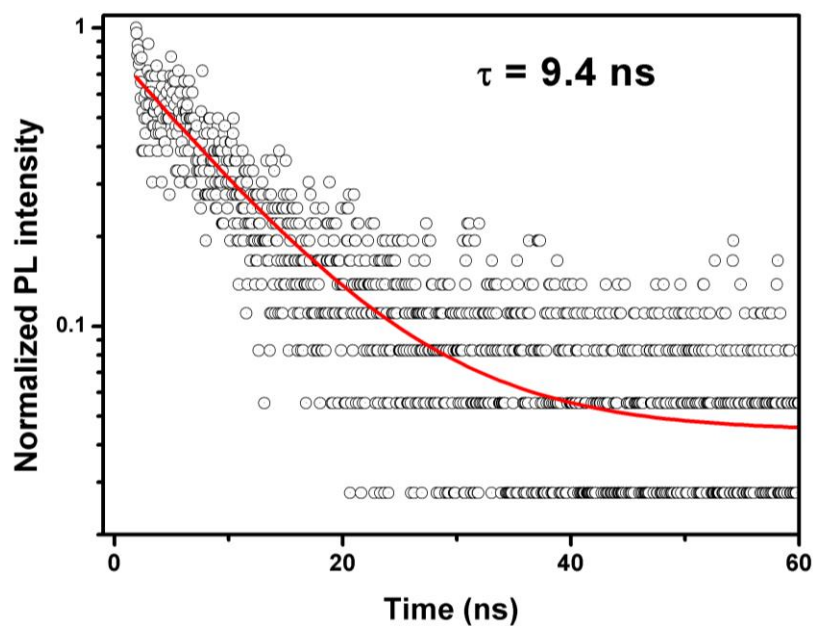


**Figure S21.** Fluorescence lifetime of **1**@MCM-41. This sample only have one processes: a long-lived component ( $\tau = 9.4$  ns). Compared with **1**@KIT-6 and **1**@SBA-15, the short-life and intermediate-life processes of nanocrystals in **1**@MCM-41 have not been observed, which may be due to the size of nanocrystals in **1**@MCM-41 is smaller than that of **1**@KIT-6 and **1**@SBA-15 samples.